Observational study

Clin Ter 2024; 175 (2):112-117 doi: 10.7417/CT.2024.5042

Tumefactive Primary Central Nervous System Vasculitis: Dynamic Susceptibility Contrast Perfusion-Weighted Magnetic Resonance Imaging Findings With Histological Correlation

C. F. Muccio[1], L. Di Lorenzo[2], G. Lepore[3], F. Savarese[1], S. Schipani[1], I. Chiarotti[4], A. Cerase[4]

[1]Unit of Neuroradiology, Department of Neurosciences, "San Pio" Hospital, Benevento, Italy; [2]UO Riabilitazione, CMR SpA, Sant'Agata dei Goti, Neuromed network Pozzilli, Italy; [3]Unit of Pathology, "San Pio" Hospital, Benevento, Italy; [4]Department of Neurological and Motor Sciences, Azienda Ospedaliero-Universitaria Senese, Policlinico "Santa Maria alle Scotte", Siena, Italy

Abstract

Purpose. Primary central nervous system vasculitis (PCNSV) is a rare inflammatory disease affecting the central nervous system. In some cases, it presents with large, solitary lesion with extensive mass effect that mimic intracranial neoplasms. This condition results in a diagnostic confusion for neuroradiologists because the differentiation is almost impossible on conventional MRI sequences. The aim of this study is to reveal the significance of dynamic susceptibility contrast (DSC) perfusion-weighted imaging in differentiating of tumefactive PCNSV (t-PCNSV) lesions from intracranial neoplasms such as glioblastomas and metastasis.

Methods. In this retrospective study, DSC of 8 patients with biopsy-proven t-PCNSV has been compared with DSC obtained in 10 patients with glioblastoma, 10 patients with metastasis, who underwent surgery and histopathological confirmation. The ratio of relative cerebral blood volume (rrCBV) was calculated by rCBV (lesion) / rCBV (controlateral normal-appearing white matter) in the gadolinium-enhancing solid areas.

Results. The mean rrCBV was 0.86±0.7 (range: 0.76-0.98) in the patients with t-PCNSV, 5,16±0.79 in patients with glioblastoma (range: 3.9-6.3), and 4.27±0.73 (range: 2.8-5.3) in patients with metastases.

Conclusion. DSC-PWI seems to be useful in the diagnostic work-up of t-PCSNVs. A low rrCBV, i.e. a rCBV similar or lower to that of the contralateral normal white matter, seems to be consistent with the possibility of t-PCSNV. ***Clin Ter 2024; 175 (2):112-117 doi: 10.7417/CT.2024.5042***

Keywords: *Brain vasculitis, Mri vasculitis, Tumefactive Central Nervous System Vasculitis*

Introduction

Primary Central Nervous System Vasculitis (PCNSV) is an enigmatic inflammatory disorder specifically targeting the blood vessels of the brain parenchyma and leptomeninges (1-3). Its aetiology remains unknown, and its diagnosis and differentiation from other conditions pose significant challenges. PCNSV is an exceedingly rare form of vasculitis, with an estimated incidence rate of 1-2.4 cases per 1,000,000 individuals annually in Europe and the United States (4,5). Notably, approximately 5%-29% of PCNSV cases present with "mass-like" lesions that can mimic neoplasms, termed tumefactive PCNSV (t-PCNSV)(6). These mass-like lesions can confound the diagnostic process, especially for neuroradiologists and clinicians. Magnetic Resonance Imaging (MRI) often reveals features suggestive of intracranial neoplasms or tumefactive demyelinating lesions, which, if not accurately diagnosed, can lead to unnecessary neurosurgery (7-9).

Dynamic Susceptibility Contrast (DSC) perfusion-weighted imaging, a magnetic resonance technique, offers insights into cerebral hemodynamics under both normal and pathological conditions. This method relies on the rapid passage of paramagnetic contrast agents, causing a reduction in T2 or T2* signal intensity proportional to tissue capillary density (10). However, DSC primarily provides relative values of cerebral blood volume (CBV) compared to contralateral normal brain tissue. Recent advancements in technology and the growing expertise of neuroradiologists have led to the increasing utilization of DSC in clinical practice.

Despite its potential, only a limited number of studies have explored the accuracy of DSC in diagnosing t-PCNSV (6,11,13), and only one case report has investigated the value of relative CBV (rCBV)(14). This case series aims to investigate the role of DSC in a relatively extensive cohort of t-PCNSV cases observed within a single institution. Additionally, it aims to compare rCBV values between t-PCNSV and other brain tumors, such as glioblastoma, metastases, and primary central nervous system lymphoma.

Patients and Methods

This retrospective study examined brain MRI and DSC studies from eight patients with confirmed t-PCNSV, verified

Correspondence: Di Lorenzo L. email: dilorenzolu@gmail.com

ISSN 1972-6007

through brain biopsy, between June 2005 and September 2022 at a single institution. These results were compared with data from ten patients with glioblastomas and ten patients with metastases who underwent surgery during the same period. The MRI inclusion criteria for glioblastomas and metastases were similar, requiring evidence of a single supratentorial gadolinium-enhancing lesion and the availability of histopathology.

Brain MRI and DSC were conducted using a 1.5T system (SignaExcite, General Electric, Waukesha WI , USA). The imaging protocol included unenhanced T1-weighted, T2-weighted, fluid-attenuated inversion recovery (FLAIR), DSC-PWI, and gadolinium-enhanced T1-weighted axial images. DSC-PWI was performed using a T2-weighted echoplanar spin-echo sequence, and post-processing was carried out using dedicated software. rCBV was calculated as a ratio of lesion rCBV to contralateral white matter rCBV. None of the t-PCNSV patients underwent digital subtraction angiography (DSA).

Results

Table 1 summarizes demographics, lesion locations, rrCBV values, and histological diagnoses for the study cohort. The t-PCNSV group consisted of six females and two males, with ages ranging from 31 to 72 years. Lesions were predominantly found in the frontal, temporal, and parietal lobes, as well as the nucleo-capsular region. Histopathology revealed four lymphocytic and four necrotizing t-PCNSV cases. The rrCBV values in t-PCNSVs ranged from 0.76 to 0.98 (mean: 0.86±0.07), distinctly lower than values observed in glioblastomas and metastases, with no overlap between the groups .

Discussion

PCNSV is an uncommon central nervous system disease of unknown etiology characterized by inflammation of the blood vessels supplying the brain parenchyma, without any evidence of systemic vasculitis (8). Inflammatory infiltration is typically composed of lymphocytes and quite frequently of granulomas, affecting the medium and small vessels supplying the brain parenchyma leading to a thickening of vessels walls (15). These changes may induce blood vessels rupture and haemorrhage or alternating segment of stenosis and occlusions with parenchymal ischemic changes of varying age (6, 15). As a result, hemorragic or ischemic presentations result in typical neuroradiological findings, despite these are not specific of PCNSV.

Table 1. Demographics, location, perfusion-weighted imaging (PWI) and diagnosis findings of the 28 patients

Patient	Sex	Age (years)	Location	PWI (rrCBV)	Diagnosis
1	F	46	Temporal	0.78	PCNSV (lymphocytic)
2	F	31	Temporal	0.76	PCNSV (necrotizing)
3	F	34	Frontal	0.90	PCNSV (necrotizing)
4	F	63	Temporal	0.98	PCNSV (lymphocitic)
5	M	52	Nucleo Capsular	0.96	PCNSV (lymphocitic)
6	F	37	Frontal	0.80	PCNSV (lymphocitic)
7	F	72	Frontal	0.88	PCNSV (necrotizing)
8	M	50	Parietal	0.86	PCNSV (necrotizing)
9	F	48	Temporal	5.70	Glioblastoma
10	M	54	Frontal	4.80	Glioblastoma
11	M	52	Temporal	6.10	Glioblastoma
12	M	65	Frontal	5.90	Glioblastoma
13	M	78	Frontal	5.10	Glioblastoma
14	M	32	Nucleo Capsular	4.45	Glioblastoma
15	M	73	Temporal	5.80	Glioblastoma
16	F	60	Frontal	4.25	Glioblastoma
17	M	60	Temporal	5.40	Glioblastoma
18	F	46	Frontal	3.90	Glioblastoma
19	F	56	Frontal	4.00	Metastasis (ovary)
20	F	62	Frontal	2.80	Metastasis (lung)
21	M	70	Frontal	4.40	Metastasis (lung)
22	F	64	Frontal	4.15	Metastasis (breast)
23	F	30	Temporal	3.95	Metastasis (breast)
24	M	55	Parietal	4.84	Metastasis (lung)
25	M	63	Frontal	3.75	Metastasis (lung)
26	M	62	Frontal	5.20	Metastasis (bladder)
27	M	61	Parietal	4.37	Metastasis (lung)
28	M	61	Frontal	5.30	Metastasis (lung)

rrCBV ratio of relative cerebral blood volume

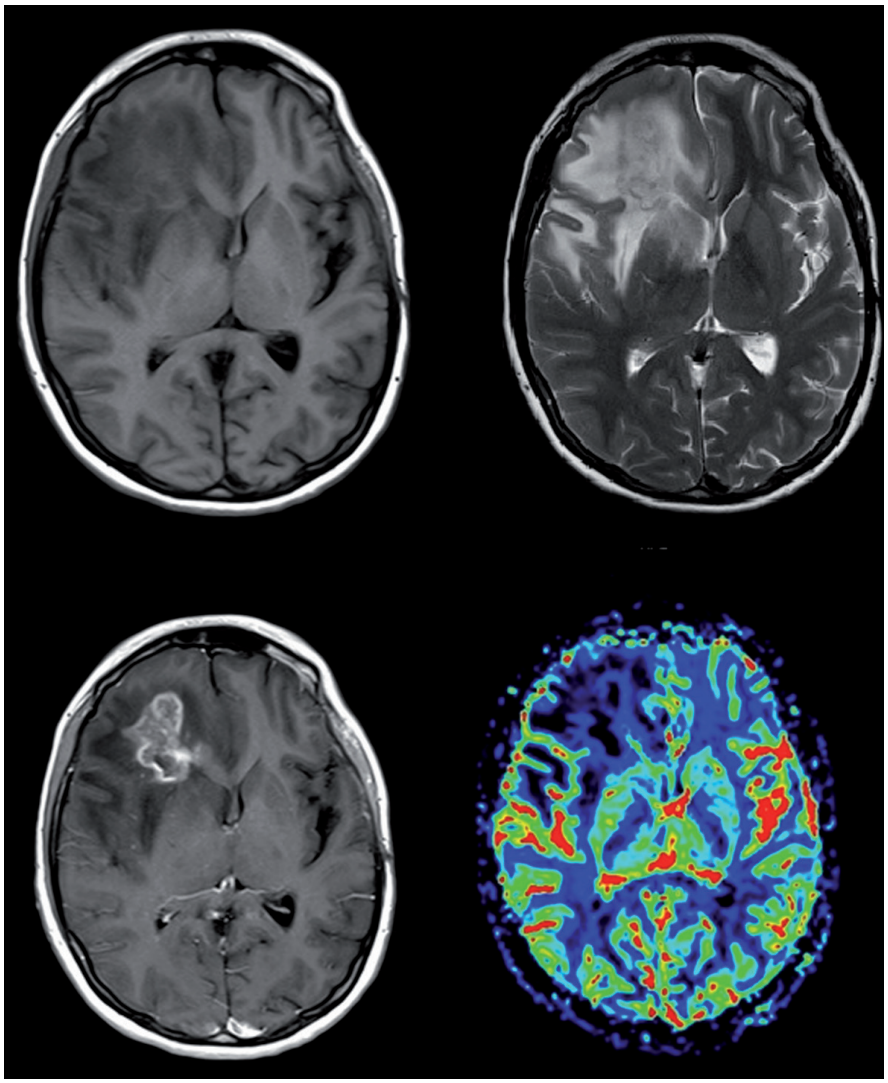

Fig.1 Common MRI features of t-PCNS. Unenhanced T1-weighted (a), gadolinium-enhanced T1-weighted (b) and T2-weighted assial MR images show a right frontal necrotic mass lesion. The mass have heterogeneous enhancement surrounded by a vasogenic edema. CBV map (c) does not show an increased rCBV in the lesion wall (arrow) and perilesional area when compared to normal controlateral white matter

The diagnosis of PCNSV is difficult because there are not specific clinical features and no laboratory or neuroimaging investigations that can confirm the diagnosis. Clinical presentation of PCNSV is highly variable with neurological disorders and symptoms such as ischemic or hemorrhagic stroke, headache, seizures, and cognitive impairment. A clinical-neuroradiological screening algorithm to move the first step towards PCNSV diagnosis has been proposed (3), but it needs to be validated.

The demonstration of the underlying vascular pathology requires to investigate intracranial arteries.

Computed tomography angiography (CTA) and MR angiography (MRA) are suitable for the detection of large- and medium-sized proximal arterial lesions, but these tecniques may not detect lesions of medium-sized vessels. Spatial resolution of modern multi-detector CTA depends on detector row thickness and is approximately 0.4–0.75 mm, while MRA spatial resolution are even less precise (17).

Compressed-sensing black-blood MRI offers promising potential in the context of neurovascular vessel wall imaging (18, 19). A 3D fast spin-echo T1-weighted sequence with variable flip-angle acquisition has been demonstrated to be a suitable technique for intracranial neurovascular vessel wall imaging and has been recently recommended by the American Society of Neuroradiology as a useful diagnostic tool for different intracranial vasculopathies (19), due to a resolution of 0.4–0.8 mm and the capacity of blood suppression. This may be helpful in the differentiation among various causes of intracranial arterial narrowing, in particular large and medium-vessel vasculitis (18).

Arteriographic diagnosis of vasculitis is based on the demonstration of one or multiple stenosis of brain vessels and microaneurysms (16). DSA provides the best evidence of vascular abnormality involving the large- and medium-sized intracranial arteries, but escapes detection of small-sized brain arteries involved in inflammatory changes. Notably, DSA resolution cannot depict the vessels disease involved in PACNSV when the vessels are <0.2 mm (9); thus, it would not be of additional diagnostic value in most PACNSVs, since most cases present with small vessels disease (20). Up to 47% of patients with PCNSVs had a positive biopsy but a normal cerebral angiogram (21).

Notably, brain biopsy is still considered the gold standard to establish the diagnosis of PCNSV (15), though there is no consensus on timepoint, surgical method and anatomical location of tissue sampling, i.e. brain tissue and/or meninges

(20). Angiography-negative, biopsy-proven PCNSV appears to be a distinct subtype of vasculitis with involvement of small intracranial vessels (21). In contrast, angiographically definite PACNSV with negative biopsy may be explained by vasculitic changes limited to proximal or medium-sized intracranial vessels which are not covered by brain biopsy (21).

Since a negative angiogram cannot exclude PACNSV (13), there are little data that may guide the choice of the optimal diagnostic approach in suspected PCNSV (22). Proton MR spectroscopy has been applied in the assessment of a variety of pathologic processes that affect the central nervous system. A spectroscopy pattern of elevated glutamate and/or glutamine peaks were reported only in three cases of PCNSV, the local accumulation of which was associated with the inflammatory processes (11,12,23).

Within these context, some PCNSVs present as solitary, supratentorial lesion, with defined borders, central necrosis, contrast-enhancement, peripheral vasogenic edema, and mass effect, i.e. a t-PCNSV. These may simulate intracranial neoplasms or tumefactive demyelinating lesions (TDL) (3, 24) disease at conventional MRI. Diagnostic correctness and speed are fundamental, given the lesions have a different prognosis and treatment.

Contrast agents are of limited usefulness, since any pathologic process associated with disruption of blood-brain barrier can result in enhancement (25). Notably, gadolinium-enhanced MR images of t-PCNSVs demonstrate various contrast pattern including patchy parenchymal enhancement, small nodular enhancement, and ring enhancement (6).

Gadolinium-enhanced susceptibility weighted imaging has been recently proposed for the diagnosis of t-PCNSV. Fonseca et al. have reported that it is possible to identify the "silver ring sign", a perivascular annular area of enhancement surrounding the small-size vessel vasculitis (26). However, further research is necessary to determine sensitivity and specificity of susceptibility weighted imaging in t-PCNSV.

DSA remains of limited value, since negative angiograms cannot rule outs the disease (13).

DSC is a noninvasive technique which provides information about cerebral haemodynamics. In intracranial lesions, MR signal increase during and after intravenous gadolinium administration is associated with the rupture of the blood-brain barrier, yet dependent on the microvascularity of the lesions themselves (9). The calculation of rCBV can therefore be used to identify and quantify the vascularization. Thus, DSC can reflect additional information about hypo- or hyperperfusion of the lesions, eventually resulting from prominent angiogenesis in neoplasms.

A t-PCNSV presenting as a ring-enhancement lesion may be difficult to differentiate from high-grade glioms, solitary metastasis when no primary cancer is known, or primary central nervous system (Table 2).

Yang el al. have reported a mean rrCBV of 6.10±3.98 in high-grade gliomas (27). Shin et al. have found this number as 4.91±1.81 (28). Aronen et al., Knopp et al., Law et al. and Sugahara et al. have reported a mean rrCBV for high-grade gliomas as 5.07, 3.64, 5.18 and 7.32 (29-32).

Calli et al. have published their results, stating that they have found rrCBV as 3.66±1.79 in anaplastic astrocytomas and 6.33±2.03 in high-grade gliomas, as well as Preul et al. have found values of rrCBV as 4.0±1.2 and 10.3±3.3 respectively (33, 34).

Table 2. Values reported for different conditions: Data provide a concise summary of the mean rrCBV values reported for high-grade gliomas, anaplastic astrocytomas, metastases, and t-PCNSV lesions from the respective studies

Condition	Study	Mean rrCBV Value
High-grade Gliomas	Yang et al.	6.10±3.98
High-grade Gliomas	Shin et al.	4.91±1.81
High-grade Gliomas	Aronen et al.	5.07
High-grade Gliomas	Knopp et al.	3.64
High-grade Gliomas	Law et al.	5.18
High-grade Gliomas	Sugahara et al.	7.32
Anaplastic Astrocytomas	Calli et al.	3.66±1.79
Anaplastic Astrocytomas	Calli et al.	6.33±2.03
Anaplastic Astrocytomas	Preul et al.	4.0±1.2
Anaplastic Astrocytomas	Preul et al.	10.3±3.3
Metastases	Hakyemez et al.	5.27±3.22
Metastases	Calli et al.	4.45±1.87
Metastases	Cho et al.	8.34±3.02
T-PCNSV Lesions	Our study	0.86±0.07

Hakyemez et al. have reported the rCBV measurements within the tumor in twenty-five patients with metastases ranging from 1.53 to 15.2 (mean: 5.27±3.22) (35). Calli et al. and Cho et al. have reported a mean rCBV from solid enhancing part of metastasis as 4.45±1.87 or 8.34±3.02, respectively (33, 36).

In our study involving 8 patients with t-PCNSV lesions, the mean rrCBV value was 0.86±0.07, thus lower than the value for both glioblastomas and cerebral metastases. This seems a clear correlation with hypoperfusion resulting from medium- and small-size arteries inflammation and the absence of neovascularization in contrast to the angiogenesis seen in tumors.

TDLs can also present with elevated rCBV values, which allows differentiation of TDL from t-PCNSV. Hiremath et al. (37) have reported the mean rCBV in TDL of 2.11 ± 1.12, similar to findings of Blasel et al. (38) who reported high rCBV with a mean of 2.89 ± 1.79 and maximum of 6.74.

Concluding, as seen, in previous MR perfusion studies TDL usually showed rCBV values ranging from 0.22 to 1.79 (39, 40), making difficult the differentiation from t-PCNSV. The elevation of CBV in TDL can presumably be explained by inflammation-related vasodilation in the acute stage, whereas the decreased perfusion in later stages of the lesion might be due to the development of a hypometabolic gliotic scar (38). However, conventional MRI features of TDL, including an open ring enhancement, a relative lack of mass effect, less substantial perifocal edema, vessels traversing through the lesion may strongly suggest the diagnosis TDL (40). Furthermore, epidemiological data including younger age and female sex, are in favour of TDL. Surely, further studies comparing DSC of t-PCNSV with that of TDL are needed.

Conclusion

In conclusion, this study suggests a potentially valuable role for DSC in diagnosing t-PCNSVs. The results demonstrate that rrCBV values in t-PCNSVs are significantly lower than those in high-grade gliomas and metastases. This observation correlates with hypoperfusion due to inflammation in medium- and small-sized arteries and the absence of neovascularization. While further research is needed to confirm these findings and validate DSC's utility in t-PCNSV diagnosis, this study contributes to our understanding of this rare and challenging condition. The study's limitations include its retrospective nature and the relatively small sample size from a single institution.

Compliance with Ethical Standards:

The study treatments were conducted according to ethical principles and was responsive to all applicable guidelines for good clinical practice

Funding:
none

Conflict of Interest:

none

Ethical approval (IRB):

study approved and conducted according all ethical principles.

Informed consent:

obtained

References

1. Ruiz-Nieto N, Aparicio-Collado H, Segura-Cerdá A, et al. Primary central nervous system vasculitis: A diagnostic and therapeutic challenge. A series of 7 patients. Neurologia (Engl Ed). 2023 Apr 28:S2173-5808(23)00026-3. doi: 10.1016/j.nrleng.2023.04.004. Epub ahead of print. PMID: 37120106.
2. Agarwal A, Sharma J, Srivastava MVP, et al. Primary CNS vasculitis (PCNSV): a cohort study. Sci Rep. 2022 Aug 5;12(1):13494. doi: 10.1038/s41598-022-17869-7. PMID: 35931755; PMCID: PMC9355950.Sarti C, Picchioni A, Telese R, Pasi M, Failli Y, Pracucci G, Cammeli D, Inzitari D (2020) "When should primary angiitis of the central nervous system (PACNS) be suspected?": literature review and proposal of a preliminary screening algorithm. Neurol Sci 41:3135-3148
3. Salvarani C, Brown RD Jr, Hunder GG. Adult primary central nervous system vasculitis: an update. Curr Opin Rheumatol. 2012 Jan; 24(1):46-52
4. Scolding NJ, Wilson H, Hohfeld R, et al. The recognition, diagnosis and management of cerebral vasculitis: a Europe survey. Eur J Neurol 2002; 9:343-347
5. Suthiphosuwan S, Bharatha A, Hsu CC-T, et al. Tumefactive primary central nervous system vasculitis: imaging findings of a rare and underrecognized neuroinfiammatory disease. AJNR Am J Neuroradiol 2020; 41:2075-2981
6. Ekmekci O, Eraslan C. Silent tumefactive demyelinating lesions and radiologically isolated syndrome. Case Rep Neurol Med 2018; 28:8409247
7. Jewells VL, Latchaw LE. CNS Vasculitis - An overview of this multiple sclerosis mimic: clinical and MRI implications. Semin Ultrasound CT MR 2020; 41:296-308
8. Jin H, Qu Y, Guo ZN, et al. Primary angiitis of the central nervous system mimicking glioblastoma: a case report and literature review. Front Neurol 2019; 10:1208
9. Muccio CF, Esposito G, Bartolini A, et al. Cerebral abscesses and necrotic cerebral tumors: differential diagnosis by perfusion-weighted magnetic resonance imaging. Radiol Med 2008; 113:747-757
10. Muccio CF, Di Blasi A, Esposito G, et al. Perfusion and spectroscopy magnetic resonance imaging in a case of lymphocytic vasculitis mimicking brain tumor. Pol J Radiol 2013; 78:66-69
11. Lee JS, Jung TY, Lee KH, et al. Primary central nervous system vasculitis mimicking a cortical brain tumor: a case report. Brain Tumor Res Treat 2017; 5:30-33
12. Yuh WTC, Ueda T, Maley JE. Perfusion and diffusion imaging: a potential tool for improved diagnosis of CNS vasculitis. AJNR Am J Neuroradiol 1999; 20:87-89
13. Muccio CF, Tedeschi E, Elefante A, et al. Primary central nervous vasculitis mimicking a brain tumor on conventional magnetic resonance imaging: the usefulness of perfusion-weighted imaging. A case report. Acta Neurol Belg 2020 ; 120:475-477
14. Giannini C, Salvarani C, Hunder G, et al. Primary central nervous system vasculitis: pathology and mechanisms. Acta Neuropathol 2012; 123:759-772
15. Küker Wilhelm. Cerebral vasculitis: imaging signs rivisites Neuroradiol 2007; 49:471-479
16. Davis AJ. Imaging of the neurovasculitides. In: Saba L, Raz E (ed) Neurovascular Imaging. Springer, New York, 2016; 683-717
17. Guggenberger K, Krafft AJ, Ludwig U, et al. High-resolution compressed-sensing T1 black-blood MRI. A new multipurpose sequence in vascular neuroimaging? Clin Neuroradiol. 2019; https://doi.org/10.1007/s00062-019-00867-0
18. Mandell DM, Mossa-Basha M, Quiai Y, et al. Intracranial vessel wall MRI: principles and expert consensus recommendations of the American Society of Neuroradiology. AJNR Am J Neuroradiol 2017; 38:218-229
19. Stoecklein VM, Kellert L, Patzig M, et al. Extended stereotatic brain biopsy in suspected primary central nervous system angiitis: good diagnostic accuracy and high safety. J Neurol 2021; 268:367-376
20. Krawczyk M, Barra LJ, Sposato LA, et al. Primary CNS vasculitis: a systematica review on clinical characteristics associated with abnormal biopsy and angiography. Autoimmin Rev 2021; 20:102714
21. Schuster S, Bachmann H, Thom V, et al. Subtypes of primary angiitis of the CNS identified By MRI patterns reflect the size of affected vessels. J Neurol Neurosurg Psychiatry 2017 ; 88:749-755
22. Beppu T, Inoue T, Nishimoto H, et al. Primary granulomatous angiitis of the central nervous system: findings of magnetic resonance spectroscopy and fractional anisotropy in diffusion tensor imaging prior to surgery. Case report. J Neurosurg 2007; 107:873-877
23. Lucchinetti CF, Gavrilova RH, Metz I, et al. Clinical and radiographic spectrum of pathologically confrmed tumefactive multiple sclerosis. Brain 2008; 131:1759-1775
24. Ferré JC, Shiroishi MS, Law M. Advanced techniques using contrast media in neuroimaging. Magn Reson Imaging Clin

N Am 2012; 20:699-713
25. Fonseca APA, do Carmo RL, Pacheco FT, et al. Primary angiitis of the CNS with unremarkable vessel wall MR imaging: how the "T1 shinethrough" effect on SWI adds to the detection of gadolinium enhancement of small intraparenchymal brain vessels. AJNR Am J Neuroradiol. 2021; https//doi: 10.3174/ajnr.A6973
26. Yang D, Korogi Y, Sugara T, et al. Cerebral gliomas: prospective comparison of multivoxel 2D chemical-shift imagin proton MRspectroscopy, echoplanar perfusion and diffusion-weighted MRI. Neuroradiology 2002; 44:656-666
27. Shin JH, Lee HK, Kwun BD, et al. Using cerebral blood flow and volume to evaluate the histopathologic grade of cerebral glioma: preliminary results. AJR Am J Roentgenol 2002; 17:783-789
28. Aronen HJ, Gazit IE, Louis DN, et al. Cerebral blood volume maps of gliomas: comparison with tumor grade and histologic findings. Radiology 1994; 191:41-51
29. Knopp EA, Cha S, Johnson G, et al. Glial neoplasm: dynamic contrast-enhanced T2*-weighted MR imaging. Radiology 1999; 211:791-798
30. Law M, Yang S, Wang H, et al. Glioma grading: sensitivity, specificity, and predictive values of perfusion MR imaging and proton MR spectroscopy imaging compared with conventional MR imaging. AJNR Am J Neuroradiol 2003; 24:1989-1998
31. Sugahara T, Korogi T, Kochi M, Usefulness of diffusion-weighted MRI with echo-planar technique in the evaluation of cellularity in gliomas. J Magn Reson Imaging 1999; 9:53-60
32. Calli C, Kitis O, Yunten N, et al. Perfusion and diffusion MR imaging in enhancing malignant cerebral tumors. Eur J Radiol 2006; 58:394-403
33. Preul C, Kuhn B, Lang EW, et al. Differentiation of cerebral tumors using multi-section echo-planar MR perfusion imaging. Eur J Radiol 2003; 48:244-251
34. Hakyemez B, Erdogan C, Bolca N, et al. Evaluation of different cerebral mass lesions by perfusion-weighted MR imaging. J Magn Reson Imaging 2006; 24:817-824
35. Cho SK, Na DG, Ryoo JW, et al. Perfusion MR imaging: clinical utility for the differential diagnosis of various brain tumors. Korean J Radiol 2002; 3:171-179
36. Hiremath SB, Muraleedharan A, Kumar S, et al. Combining diffusion tensor metrics and DSC perfusion imaging: can it improve the diagnostic accurancy in differentiating tumefactive demyelination from high-grade glioma? AJNR Am J Neuroradiol 2017; 38:685-690
37. Blasel S, Pfeilschifter W, Jansen V, et al. Metabolism and regional cerebral blood volume in autoimmune inflammatory lesions demyelinating lesions mimicking malignant gliomas. J Neurol 2011; 258:113-122
38. GE Y, Law M, Johnson G, et al. Dynamic susceptibility contrast perfusion MR imaging of multiple sclerosis lesions: characterizing hemodynamic impairment and inflammatory activity. AJNR Am J Neuroradiol 2005; 26:1539-1547
39. Wuerfel J, Bellmann-Strobl J, Brunecker P, et al. Changes in cerebral perfusion precede plaque formation in multiple sclerosis: a longitudinal perfusion MRI study. Brain 2004; 127:111-119
40. Naik S, Bhoi SK, Agarwal V, et al. Perfusion MR may facilitate the diagnosis of a tumefactive demyelinating lesion. Neurol India 2019; 67:908-910